Journal of Chemistry and Technologies, 2024, *32*(1), 9-16

Journal of Chemistry and Technologies

pISSN 2663-2934 (Print), ISSN 2663-2942 (Online).

journal homepage: http://chemistry.dnu.dp.ua
*editorial e-mail:*chem.dnu@gmail.com

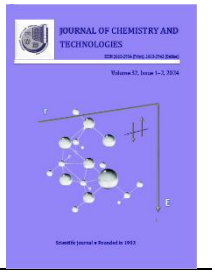

UDC 661.097.3

A FIRST-PRINCIPLES STUDY EFFECT PRESSURE OF ELECTRONIC AND OPTICAL PROPERTIES OF R-TiO_2

Abdulhadi M. Ghaleb[1*], Yamina Benkrima[2], Rafea A. Munef[1], Ahmed Th. Shihatha[1], Yousra Megdoud[3], Zahraa Talib Ghaleb[4]

[1]*Department of Physics, College of Science, University of Kirkuk, Iraq*
[2]*Department of Exact Sciences, ENS Ouargla, Algeria*
[3]*Institute of Sciences, Centre University Morsli Abdallah Tipaza, Algeria*
[4]*Department Chemistry, College of Science, Kirkuk University, Kirkuk, Iraq*

Received 15 October 2023; accepted 7 December 2023; available online 25 April 2024

Abstract

The band structure, density of state, and optical properties of TiO_2 rutile were studied using first principles calculations within the framework of density functional theory using the generalized gradient approximation (GGA-RPBE) at both zero and high pressures. we used the Birch-Murnaghan equation of state calculate of volume and bulk modulus by approximation that we mentioned above and our results were compared with previous theoretical and experimental data, we noticed a good agreement between the results. The band gap of 2.098 eV (GGA) remains unchanged when the pressure is increased from 0 to 10 GPa, indicating an underestimation. The reduction in volume and lattice constants with increasing pressure is responsible for the decrease in band gap. There is a good agreement between the experimental results and the dielectric constant ε (ω) and refractive index. The photocatalytic activity of TiO_2 is found to decrease with increasing pressure based on the absorption spectrum. The energy loss spectra show new peaks as a result of the pressure effect on the energy loss function. From our results, we noticed the effect of pressure within the range (0–60 GPa) on each of the structural, electronic and optical properties, and there is also good agreement between the current results and previous results.

*Keywords:*first principle; Ultrasoft pseudopotential; Density of states; Refractive index; Hydrostaticpressure.

ПЕРВИННЕ ДОСЛІДЖЕННЯ ЕФЕКТУ ВПЛИВУ ТИСКУ НА ЕЛЕКТРИЧНІ ТА ОПТИЧНІ ВЛАСТИВОСТІ РУТИЛУ TiO_2

Абдулхаді М. Галеб[1], А. Ю. Бенкріма[2*], Рафеа А. Мунеф[1], Ахмед Т. Шихатха[1], Юсра Мегдуд[3], Захра Таліб Галеб[4]

[1]*Кафедра фізики, Науковий коледж, Університет Кіркука, Кіркук, Ірак*
[2]*Департамент точних наук, ENS Уаргла, Алжир*
[3]*Інститут наук, Центральний університет Морслі Абдалла Тіпаза, Алжир*
[4]*Кафедра хімії, Коледж науки, Університет Кіркук, Кіркук, Ірак*

Анотація

Електронні константи, оптичні властивості та показники пружності рутилу TiO_2 досліджено з використанням першого принципу. Ефекти обмінної кореляції з використанням RPBE описано в термінах узагальненого градієнтного наближення [GGA]. Виміряні об'єм та об'ємний модуль добре узгоджуються з попередніми експериментальними і теоретичними результатами. Розраховано ширину забороненої зони (2.098 еВ) з урахуванням більшої інтенсивності станів і розширенними енергетичними зонами навколо рівнів Фермі. Діелектричну проникність визначено з урахуванням електронної зонної структури і, з огляду на її важливість, використано для обчислення решти оптичних властивостей, таких як функція втрат енергії, показник заломлення, поглинання і відбивання. Вплив гідростатичного тиску (0–60 ГПа) показано на змінах властивостей. Результати нашого дослідження добре узгоджуються з відомими сучасними експериментальними і теоретичними результатами.

Ключові слова: перший принцип; надм'який псевдопотенціал; густина станів; показник заломлення; гідростатичний тиск.

**Corresponding author: e-mail: abdlhadig4@gmail.com*

doi: 10.15421/jchemtech.v32i1.289257

Journal of Chemistry and Technologies, 2024, *32*(1), 9-16

Introduction

Titanium dioxide (TiO_2) is a complex transition metal oxide that is readily available and well described experimentally, with a wide range of applications [1]. TiO_2 has a wide range of industrial applications, including photoelectrodes [2], electronics [3], gas sensing, painting [4], and dye-sensitized solar cells [5]. Hence, the utilization of TiO_2 in photocatalytic processes under visible light is significantly constrained. In order to enhance the range of wavelengths that TiO_2 can respond to and its overall photo catalytic efficiency across the entire solar spectrum, extensive endeavors have been undertaken [6–8]. Although many theoretical calculations of the electronic properties of rutile TiO_2 have been reported in the literature [9–14], there are significant differences between these previously calculated values and the corresponding experimental ones. The theoretical direct band gaps range from 1.67 to 3.25 eV (for the local density approximation, LDA), 1.69 to 4.45 eV (for the generalized gradient approximation, GGA), and more than 3.4 to 13.05 eV (for the Hartree-Fock approximation, HF). We do not know of any previous reports of a calculated, fundamental, indirect band gap for rutile TiO_2. Here, we report on studies of the electronic and structural band gap of rutile titanium dioxide at various hydrostatic pressure levels using a first-principles plane-wave ultra soft pseudo-potential method. Results and a discussion are presented in the section that follows, along with the specifics of the computational approach. The conclusion of this work is presented in the last section.

Theoretical Method

The present calculations are based on the implementation of the plane wave pseudo potential of density functional theory [15; 16] using the computational program CASTEP [17], which is supported by density functional theory and molecular dynamics theory. RPBE was first proposed in 1998 with the goal of improving in the chemical absorption of energy of atoms and molecules [18]. Therefore, we adopted GGA with the RPBE as the exchange correlation function [19]. The electronic arrangement of O and Ti are $2s^2 2p^4$and $3s^2 3p^6 3d^2 4s^2$,respectively. The valence of electrons O and Ti are 4 and 6 respectively. Ultrasoft Pseudo potential (USP) has been used to define the plane wave base and to perform mathematical operations to reduce the cutoff energy with minimal contribution from the core region. The kinetic energy cutoff (400eV) was used to extend the smooth portion of the wave function in the plane wave. A 2×2×2 k-point grid is used to integrate the Brillion region for rutile TiO_2. The Broyden-Fletcher-Goldfarb-Shenno (BFGS) miniature method was used to improve the geometry [20]. The convergence of displacement was set to less than 0.001 A°, and the energy difference was set to less than 1×10^{-6} eV / atom.

Results and discussion

Electronic properties. The BFGS algorithm was used to perform the geometry optimization. For the quadrangular rutile TiO_2 compound at the experimental lattice constant a = b= 4.716818 A° and c = 2.96673A°.These equilibrium lattice constants are 1 % higher as compared to experimental values [21]. The equilibrium lattice state parametries, pressure derivative and bulk elastic modulus are presented below using Birch-Murnaghan equation [22]:

$$p(V) = 1.5B_{\circ}\left[(\frac{V_{\circ}}{V})^{\frac{7}{3}} - (\frac{V_{\circ}}{V})^{\frac{5}{3}}\right]\left\{1 + 0.75(B^{'} - 4)\left[(\frac{V_{\circ}}{V})^{\frac{2}{3}} - 1\right]\right\}, \quad (1)$$

where $B^{'}$, $B_{\circ}$ and $V_{\circ}$ are pressure derivative of bulk modulus, bulk modulus and equilibrium volume, respectively. The data in Table 1 are in good agreement with the theoretical [23–27] and experimental results[28].

Table 1

Calculate, volume ($V_{\circ}$) and bulk modulus ($B_{\circ}$) of rutileTiO_2

	$V_{\circ}[A^3]$	$B_0[GPa]$
Present work	65.7	221
Zhu Jun et al. [23]	–	258
Iuga et al. [24]	63.3	235
Basavaraj et al. [25]	–	229.1
Yao et al. [LDA,GGA] [26]	61.11;64.47	245.2, 211.3
Zhou et al . [27],	64.34	221
Al-Khatatbeh et al. [28]Exp.	62.4	235

As shown in Fig. 1(a), the energy band gap was 2.098 eV, which is 40% smaller than that of the experimental band gap Ref [29]. The band gap calculation relies on the GGA approximation and DFT, suggesting that the band

Journal of Chemistry and Technologies, 2024, *32*(1), 9-16

gap magnitude is underestimated due to the derivative of the exchange-correlation energy gap [30; 31]. The energy band gap diagram of rutile TiO_2 is illustrated in Figure 1(a). The top of valence band is chosen as the Fermi level ($E_f = 0\ eV$). The valence band maximum and conduction band minimum are observed at G point, which makes this material a direct gap (G–G) material. Some of the important features of this gap are presented in Table 2.

Table 2

Direct and indirect band gaps (eV) and their valence corresponding to the conduction band transfer of rutile TiO_2 at zero pressure

Valence to conduction band transition	Band gap energies (eV)
G–G	2.098
Z–Z	2.97
R–R	2.14
X–X	2.74
M–M	2.14
A–A	2.68

Fig. 1(b) shows the relationship between hydrostatic pressure and energy band gap with increasing pressure, the variable gap energy of rutile TiO_2 is indicated by the black dot in Fig. 1(b).

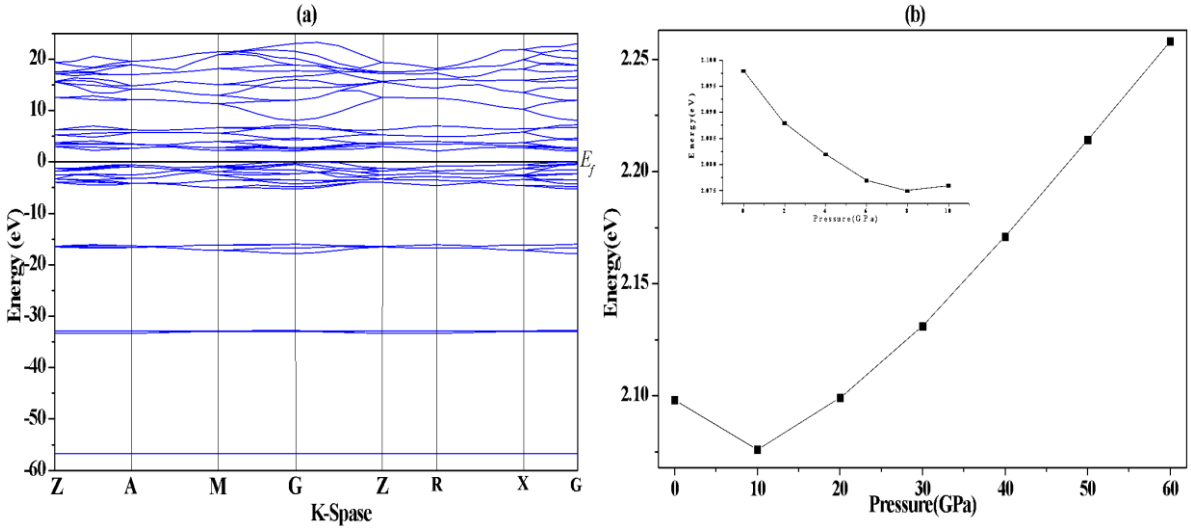

Fig. 1. a) Band structure of rutile TiO_2 at zero pressure and b) Relationship between band gap and pressure

This means that the energy gap passes through two stages: first stage falls within the range (0–8 GPa) of the applied pressure. The nonlinear relationship between energy gap and pressure, which decreases with increasing pressure, can be fitted using a third polynomial, which is expressed as:

$$E_g(p) = E_g(0)+7.394\times10^{-4}p + 1.152 \times 10^{-4}p^2 + 1.563 \times 10^{-6}p^3. \quad (2)$$

In the second stage, after 10 GPa up to 60 GPa, energy gap increases almost linearly with increasing pressure in steps of 10 GPa. These differences may be related to slow changes in the crystal structure caused by the external pressure. The results showed that the energy gap related to different electronic states expanded with increasing pressure.

In order to get a better visualization of the electronic domain structure, T DOS and PDOS plots are shown in Fig. 2 (a–f). The total density of states roughly stretches from –57.5eV to 23.3 eV, Fig. 2(a) determines the TDOS character with increasing pressure. Fig.2(b–f) PDOS shows that the contribution of (O-2p) states is dominant in VB, while (Ti-3d) states are less dominant for VB width it is 5.6eV (fig. 2a), which are in agreement with the theoretical results of Baizaee and Mousavi and the experimental results of 5.25eV and 5.4eV, respectively, [32; 33] from fig. 2 (b–f). As (Ti-d) and (O – p) states play an essential role in the construction of band conduction, from this we can conclude that transition between VB and CB is caused by the states of (O – 2p) and (Ti – 3d), since the states have maximum contribution to VB and CB. The DOS irregularity occurs in this region due to hybridization of the (O-p) orbital with the (Ti-3d) orbital. When DOS is compressed, it causes the energy gap to widen by shifting the valence band to

Journal of Chemistry and Technologies, 2024, *32*(1), 9-16

a lower energy level and the conduction band to a higher energy level. A decrease in TDOS and PDOS indicates that fewer states are available for a specified level.

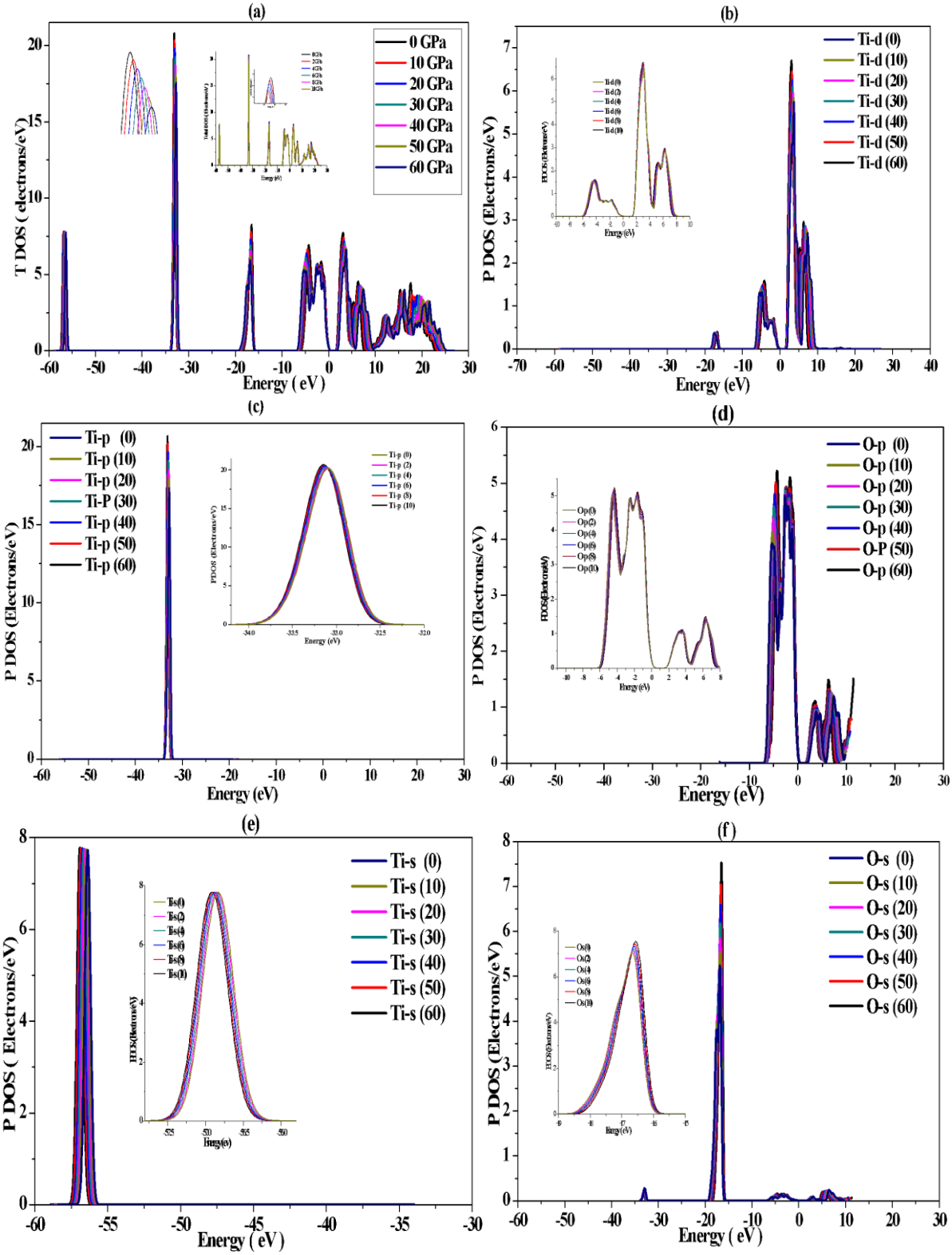

Fig. 2. a) TDOS of Rutile TiO_2, and PDOS for b) Ti-d, c) Ti-p, d) O-p, e) Ti-s and f) O-s at zero and high hydrostatic pressures

Optical properties. The most important and widely studied are the optical properties of materials, which is closely related to electronic, magnetic and thermal properties. The optical properties including refractive index, dielectric function, absorption coefficient and reflectivity obtained from light as it passes through the TiO_2 rutile were analyzed for the optimized TiO_2 rutile. Optical properties related to the complex dielectric function include conductivity, dielectric

Journal of Chemistry and Technologies, 2024, *32*(1), 9-16

constant, index of refraction, reflection and absorption. One is interconnected with the others. The electrical function is defined.

$$\varepsilon(\omega)_{=}\varepsilon_1(\omega) + i\varepsilon_2(\omega), \quad (3)$$

where:$\varepsilon_{(1)}(\omega)$,$\varepsilon_2(\omega)$ are express the real and imaginary parts of the dielectric function, respectively, in general, the dielectric function is associated with the electronic structure, the imaginary part of equation (2) is defined as follows:

$$\varepsilon_2(h\omega) = \frac{2\pi e^2}{\Omega\varepsilon_o}\sum_{k,v,c}|\langle\psi_k^c|u,r|\psi_k^v\rangle|^2\,\delta(E_k^c\text{-}E_k^v\text{-}E)\,, \quad (4)$$

where ψ_k^c and ψ_k^v, μ,e represent the wave functions of the conduction band and valence band, incident electric field, and electronic charge at point k, respectively. The Kramer-kronig relation was used to obtain the real part from the imaginary dielectric function. From fig. 3(a), it can be seen that the imaginary part of the dielectric function it starts at 1.37 eV with a first peak of 5.12 eV due to excitation from VBM to CBM, second peak 7.69 eV and third peak 12 eV. This is due to transitions from A to M and M to G and G to L respectively. The influence of hydrostatic pressure is manifested as a transformation of the imaginary part of the dielectric function (ε_2) towards larger values, as shown in Fig. 3(b). Light absorption efficiency of rutile decreases with increasing pressure. The dielectric function is important for the derivation of the other optical properties such as refractive index $(n(\omega))$, energy loss spectrum $(L(\omega))$, reflectivity $(R(\omega))$ and absorption coefficient $(\alpha(\omega))$through the specified relationships [34–36].

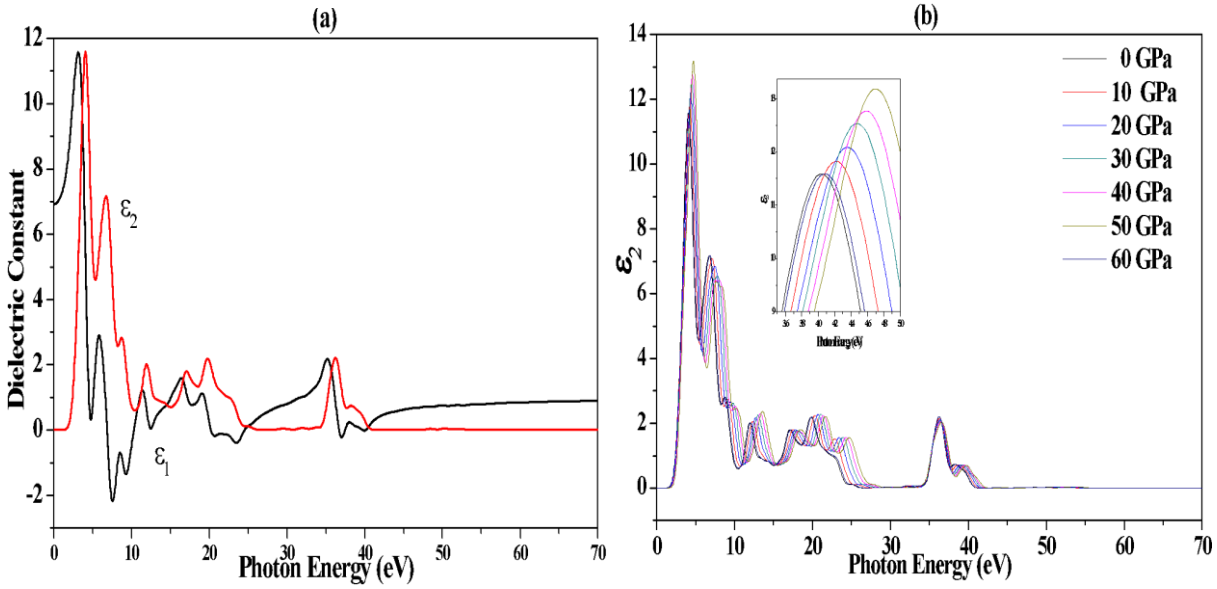

Fig. 3. Calculated a) real and imaginary part of dielectric constants at zero pressure, b) imaginary part of dielectric function (ε_2) under high pressure of rutile TiO_2

$$n(\omega) = \sqrt{\frac{|\varepsilon(\omega)|+\varepsilon_1(\omega)}{2}}; \quad (5)$$

$$L(\omega) = Im\left(\frac{-1}{\varepsilon(\omega)}\right) = \frac{\varepsilon_2(\omega)}{\varepsilon_1^2(\omega)+\varepsilon_2^2(\omega)}; \quad (6)$$

$$k(\omega) = \sqrt{\frac{|\varepsilon(\omega)|-\varepsilon_1(\omega)}{2}}; \quad (7)$$

$$R(\omega) = \frac{(n-1)^2+k^2}{(n+1)^2+k^2}; \quad (8)$$

$$\propto(\omega) = \frac{2k\omega}{c}. \quad (9)$$

From fig.4(a) it can be seen that the refractive index is 2.63 and increases with pressure. Its peak is close to the value of 3.55 (under 60GPa) at an energy of 3.27eV in UV region as shown in Fig.4(a).

Journal of Chemistry and Technologies, 2024, *32*(1), 9-16

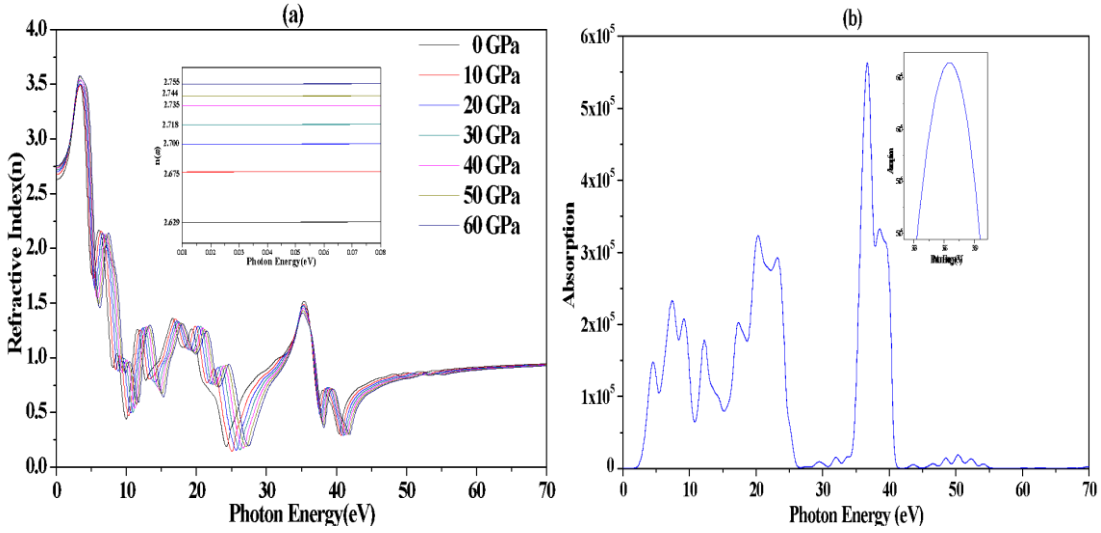

Fig. 4. Calculated a) refractive index(n(ω)) at various pressures b) the absorption coefficient ($\alpha(\omega)$) of rutile TiO_2

As for the results, they are summarized in Table 3 for the refractive index and dielectric constant., It has been compared with the existing literature [32; 37; 38]. It turns out that the value of our calculated dielectric constant is somewhat greater compared to the values of the previous theoretical calculations [32] and experimental results [37].

Table 3

Calculated values of refractive index and dielectric constant of rutile TiO_2

Method	Refractive index (n)	Dielectric constant (ε_1)
GGA-RPBE [Present work]	2.63	6.91
GGA [32]	2.65	6.58
GGA+SOC [32]	2.65	–
LDA [32]	2.7	–
LDA+SOC [32]	2.71	–
Angel-Vosko [32]	2.54	–
GGA+PBE [28]	2.61	–
Experimental [37; 38]	2.71 [38]	6.693 [37]

While the value of the refractive index agrees with experimental results [38], Fig. 4(a,b) show the achieved results of refractive index(n(ω)), absorption coefficient($\alpha(\omega)$) ,and Fig.5(a,b) show both the the energy loss function(L(ω))and reflectivity (R(ω)) and, which are a major factor to ensure full energy utilization, and their main peaks are identified in the UV region as shown in fig.5(a). The energy loss function ($L(\omega)$) is a key factor to estimate the total energy utilization, ,its main peaks are identified in the UV regions shown in Fig.5(a). They are connected by rough edges in reflection spectra as shown in Fig.5(b). From Fig.5(b), it can be seen that rutile TiO_2 is an external absorbent of visible in accordance with the explanation of the study [39]. The absorption begins in the UV region (3.1 V) and reaches a maximum at 36.6 V, where the energy loss function is the lowest.

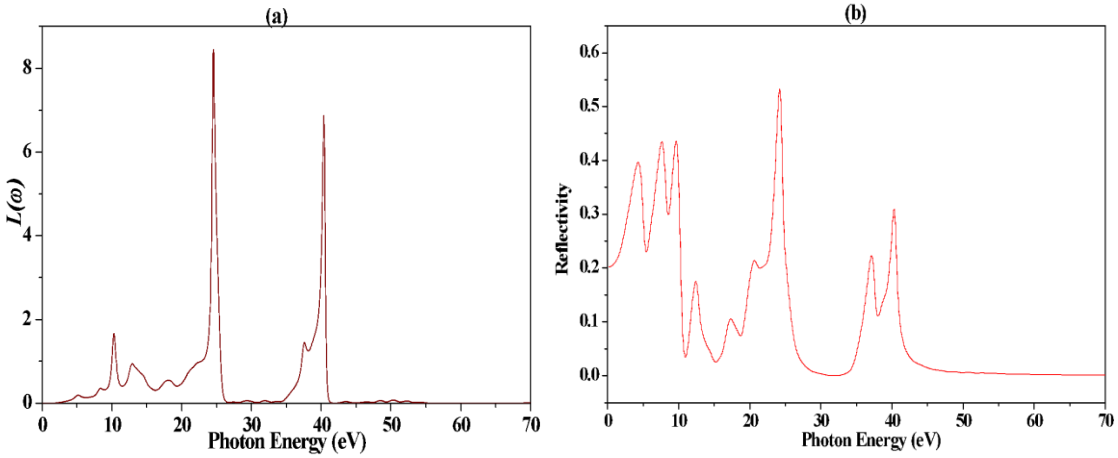

Fig. 5. Calculated a) the energy loss function (L(ω)), b) the reflectivity ($R(\omega)$)rutile TiO_2

Conclusion

We performed first principle calculations on rutile TiO_2 using the GGA-RPBE approximation combined with the Ultra soft pseudo potential method to investigate both electronic and optical properties. The approximate band gap value was 2.098 eV, which is smaller than the experimental value 3.0 eV, although this is in good agreement with other GGA-based calculations. On application of the external pressure, the direct band gap decreases in the first stage with the hydrostatic pressure from 0GPa to 8GPa and then increases in the second stage with the hydrostatic pressure from 10GPa to 60GPa. The valence bandwidth has been roughly determined to be 5.55 eV, which closely corresponds to the experimental value of 5.4 eV and is consistent with other theoretical results as well. The dielectric constant was estimated to be 6.91, which is slightly over the experimental value 6.693. Whereas, the refractive index was determined with a value of 2.63 according to the electronic band structure against the experimental value of 2.71. The effects of pressure showed that the imaginary part of the dielectric function (ε_2) shifts towards higher photon energies as the complex refractive index decreases with increasing pressure. The absorption spectrum shows that TiO2 poorly absorbs visible light and the absorption spectrum is dominated by ultraviolet light with a maximum at 36.4 eV.

References

[1] Diebold, U. (2003). The surface science of titanium dioxide. *Surface science reports, 48*(5-8), 53-229. https://doi.org/10.1016/S0167-5729(02)00100-0

[2] Long, L. L., Zhang, A. Y., Yang, J., Zhang, X., Yu, H. Q. (2014). A green approach for preparing doped TiO_2 single crystals. *ACS Applied Materials & Interfaces*, *6*(19), 16712–16720. https://doi.org/10.1021/am503661w

[3] Azer, B. B., Gulsaran, A., Pennings, J. R., Saritas, R., Kocer, S., Bennett, J. L., Yavuz, M. (2022). A Review: TiO2 based photoelectrocatalytic chemical oxygen demand sensors and their usage in industrial applications. *Journal of Electroanalytical Chemistry*, *918*, 116466. https://doi.org/10.1016/j.jelechem.2022.116466

[4] Varghese, O. K., Grimes, C. A. (2003). Metal oxide nanoarchitectures for environmental sensing. *Journal of nanoscience and nanotechnology, 3*(4), 277–293. https://doi.org/10.1166/jnn.2003.158

[5] Lazzeri, M., Vittadini, A., Selloni, A. (2001). Structure and energetics of stoichiometric TiO_2 anatase surfaces. *Physical Review B, 63*(15), 155409. https://doi.org/10.1103/PhysRevB.63.155409

[6] Nie, X., Zhuo, S., Maeng, G., & Sohlberg, K. (2009). Doping of TiO_2 Polymorphs for Altered Optical and Photocatalytic Properties. *International Journal of Photoenergy,* 2009. https://doi.org/10.1155/2009/294042

[7] Zaleska, A. (2008). Doped-TiO_2: a review. *Recent patents on engineering, 2*(3), 157–164. https://doi.org/10.2174/187221208786306289

[8] Henderson, M. A. (2011). A surface science perspective on TiO2 photocatalysis. *Surface Science Reports, 66*(6-7), 185–297. https://doi.org/10.1016/j.surfrep.2011.01.001

[9] Labat, F., Baranek, P., Domain, C., Minot, C., & Adamo, C. (2007). Density functional theory analysis of the structural and electronic properties of TiO2 rutile and anatase polytypes: Performances of different exchange-correlation functionals. *The Journal of chemical physics, 126*(15). https://doi.org/10.1063/1.2717168

[10] Morita, K., Yasuoka, K. (2018). Density functional theory study of atomic and electronic properties of defects in reduced anatase TiO_2 nanocrystals. *AIP Advances*, *8*(3). https://doi.org/10.1063/1.5021024

[11] Islam, M. M., Bredow, T., Gerson, A. (2007). Electronic properties of oxygen-deficient and aluminum-doped rutile TiO_2 from first principles. Physical Review B, 76(4), 045217. https://doi.org/10.1103/PhysRevB.76.045217

[12] Fox, H., Newman, K. E., Schneider, W. F., Corcelli, S. A. (2010). Bulk and surface properties of rutile TiO_2 from self-consistent-charge density functional tight binding. Journal of chemical theory and computation, 6(2), 499–507. https://doi.org/10.1021/ct900665a

[13] Manzoli, M., Freyria, F. S., Blangetti, N., Bonelli, B. (2022). Brookite, a sometimes under evaluated TiO_2 polymorph. *RSC Advances*, *12*(6), 3322-333. https://doi.org/ 10.1039/d1ra09057g

[14] Zhao, W., Li, Y., Shen, W. (2021). Tuning the shape and crystal phase of TiO_2 nanoparticles for catalysis. *Chemical Communications*, *57*(56), 6838–6850. https://doi.org/10.1039/D1CC01523K

[15] Milman, V., Refson, K., Clark, S. J., Pickard, C. J., Yates, J. R., Gao, S. P., Segall, M. D. (2010). Electron and vibrational spectroscopies using DFT, plane waves and pseudopotentials: CASTEP implementation. *Journal of Molecular Structure: THEOCHEM*, *954*(1-3), 22–35. https://doi.org/ 10.1016/j.theochem.2009.12.040

[16] Gao, S. P., Pickard, C. J., Perlov, A., Milman, V. (2009). Core-level spectroscopy calculation and the plane wave pseudopotential method. *Journal of Physics: Condensed Matter*, *21*(10), 104203. https://doi.org/ 10.1088/0953-8984/21/10/104203

[17] Segall, M. D., Lindan, P. J., Probert, M. A., Pickard, C. J., Hasnip, P. J., Clark, S. J., Payne, M. C. (2002). First-principles simulation: ideas, illustrations and the CASTEP code. *Journal of physics: condensed matter*, *14*(11), 2717. https://doi.org/10.1088/0953-8984/14/11/301

[18] Hammer, B. H. L. B., Hansen, L. B., Norskov, J. K. (1999). Improved adsorption energetics within density-functional theory using revised Perdew-Burke-Ernzerhof functionals. *Physical review B*, *59*(11), 7413. https://doi.org/10.1103/PhysRevB.59.7413

[19] Wen, J. Q., Zhang, J. M., Chen, G. X., Wu, H., Yang, X. (2018). The structural, electronic and optical properties of Nd doped ZnO using first-principles calculations. *Physica E: Low-dimensional Systems and Nanostructures*, *98*, 168–173. https://doi.org/10.1016/j.physe.2018.01.002

[20] Zhao, W. (2021). A Broyden–Fletcher–Goldfarb–Shanno algorithm for reliability-based design optimization. *Applied Mathematical Modelling*, *92*, 447–465. https://doi.org/10.1016/j.apm.2020.11.012

[21] Wu, S., Luo, X., Long, Y., Xu, B. (2019). Exploring the phase transformation mechanism of titanium dioxide by high temperature in situ method. In *IOP Conference Series: Materials Science and Engineering* 493(1), 012010. https://doi.org/10.1088/1757-899X/493/1/012010

[22] Birch, F. (1978). Finite strain isotherm and velocities for single-crystal and polycrystalline NaCl at high pressures and 300 K. *Journal of Geophysical Research: Solid Earth*, *83*(B3), 1257–1268. https://doi.org/10.1029/JB083iB03p01257

[23] Jun, Z., Jing-Xin, Y., Yan-Ju, W., Xiang-Rong, C., & Fu-Qian, J. (2008). First-principles calculations for elastic properties of rutile TiO2 under pressure. *Chinese Physics B*, *17*(6), 2216. https://doi.org/10.1088/1674-1056/17/6/046

[24] Iuga, M., Steinle-Neumann, G., Meinhardt, J. (2007). Ab-initio simulation of elastic constants for some ceramic materials. *The European Physical Journal B*, *58*, 127–133. https://doi.org/10.1140/epjb/e2007-00209-1

[25] Basavaraj, K., Nyayban, A., Panda, S. (2022, July). Structural phase transitions and elastic properties of TiO_2 polymorphs: Ab-initio study. In *IOP Conference Series: Materials Science and Engineering, 1248*(1), 012064. https://doi.org/10.1088/1757-899X/1248/1/012064

[26] Yao, H., Ouyang, L., Ching, W. Y. (2007). Ab initio calculation of elastic constants of ceramic crystals. *Journal of the American Ceramic Society*, *90*(10), 3194–3204. https://doi.org/10.1111/j.1551-2916.2007.01931.x

[27] Zhou, X. F., Dong, X., Qian, G. R., Zhang, L., Tian, Y., Wang, H. T. (2010). Unusual compression behavior of TiO_2 polymorphs from first principles. *Physical Review B*, *82*(6), 060102. https://doi.org/10.1103/PhysRevB.82.060102

[28] Al-Khatatbeh, Y., Lee, K. K., Kiefer, B. (2009). High-pressure behavior of TiO 2 as determined by experiment and theory. *Physical Review B*, *79*(13), 134114. https://doi.org/10.1103/PhysRevB.79.134114

[29] Naik, V. M., Haddad, D., Naik, R., Benci, J., Auner, G. W. (2002). Optical properties of anatase, rutile and amorphous phases of TiO_2 thin films grown at room temperature by RF magnetron sputtering. *MRS Online Proceedings Library (OPL)*, *755*, DD11-12. https://doi.org/10.1557/PROC-755-DD11.12

[30] Perdew, J. P., Levy, M. (1983). Physical content of the exact Kohn-Sham orbital energies: band gaps and derivative discontinuities. *Physical Review Letters*, *51*(20), 1884. https://doi.org/10.1103/PhysRevLett.51.1884

[31] Sham, L. J., Schlüter, M. (1983). Density-functional theory of the energy gap. *Physical review letters*, *51*(20), 1888. https://doi.org/10.1103/PhysRevLett.51.1888

[32] Baizaee, S. M., Mousavi, N. (2009). First-principles study of the electronic and optical properties of rutile TiO2. *Physica B: Condensed Matter*, *404*(16), 2111–2116. https://doi.org/10.1016/j.physb.2009.01.014

[33] Kowalczyk, S. P., McFeely, F. R., Ley, L., Gritsyna, V. T., Shirley, D. A. (1977). The electronic structure of SrTiO3 and some simple related oxides (MgO, Al_2O_3, SrO, TiO_2). *Solid State Communications*, *23*(3), 161–169. https://doi.org/10.1016/0038-1098(77)90101-6

[34] Liu, Q. J., Liu, Z. T., Feng, L. P., Tian, H. (2010). First-principles study of structural, elastic, electronic and optical properties of rutile GeO_2 and α-quartz GeO_2. *Solid state sciences*, *12*(10), 1748–1755. https://doi.org/10.1016/j.solidstatesciences.2010.07.025

[35] Fang, R. C. (2003). Solid spectroscopy. *Chinese Science Technology University Press, Hefei*.

[36] Zhang, Y., Shen, W. M. (2005). Basic of solid electronics. *Zhe-Jiang University Press, Hangzhou*.

[37] Davis, T. A., Vedam, K. (1968). Pressure dependence of the refractive indices of the tetragonal crystals: ADP, KDP, $CaMoO_4$, $CaWO_4$, and rutile. *JOSA*, *58*(11), 1446–1451. https://opg.optica.org/josa/abstract.cfm?URI=josa-58-11-1446

[38] Lide, D. R. (2003). *CRC Handbook of Chemistry and Physics,* 83rd edn CRC Press, Boca Raton, FL. Nielsen et al.

[39] Ghaleb, A. M., Munef, R. A., Mohammed, S. F. (2022). First principles study the effect of Zn doped MgO on the energy band gap using GGA approximation. *Journal of Ovonic Research*, *18*(1). https://doi.org/10.15251/JOR.2022.181.11